Effect of Dirt on Global Irradiation Measuring Equipment in Coastal Conditions in the Arica and Parinacota Region

L. Cornejo[1,2,3], E. Rodríguez[2], C. Flores[3], A. Cabrera-Reina[1,3]

Abstract— The aim of this study was to evaluate the effect of environmental dirt on the global irradiation measurement equipment installed in a weather station in the city of Arica, Chile, as well as characterizing the content of the settleable particulate material deposited on the station. Since it was not possible to use two pyranometers simultaneously in the elaboration of this research, the first step was to obtain a model of global irradiation using the other data available from the weather station as input variables. Calculating global irradiation by adding the direct and diffuse components is an effective method (4.5% average error), although the use of a polynomial equation allows this error to be reduced (3.5% average error). It was observed that the error in the measurement is related to the irradiation level and the presence of three characteristic zones: (i) when irradiance is below 50 W/m^2 the largest errors are present (ii) when irradiance is between 50 and 500 W/m^2 the error increases as irradiance increases (iii) above 500 W/m^2 the error stabilizes in the region of 5-6%. In addition, it was determined that the effect of dirt is negligible during the first 7 days. The minerals present in greatest proportions were identified as: Halite, Gypsum, Quartz, Albite, Anorthite and Anhydrite. All these minerals appear to be originate from natural sources of contamination such as the proximity to the Pacific Ocean and the desert conditions in the area. No mineral that may be associated with anthropogenic sources was found in any great quantity.

Index Terms— Diffuse horizontal irradiance, Dirt, Direct irradiance, Global horizontal irradiance, Pyranometer, Pyrheliometer, Weather station

1 INTRODUCTION

The development of a global economy and an increase in environmental awareness have focused attention on the use of clean energy and sustainable processes. As a result, solar systems have been applied to many areas of study, such as: construction work, treatment of contaminated water, obtaining thermal energy for desalination, solar panels for producing electricity or solar ovens, among others [1].

However, one of the main problems in the implementation of solar systems is a lack of reliable data on solar irradiation. In Arica (XV region, Chile), this situation is augmented by the fact that there is neither a typical meteorological year (TMY) nor appropriate analysis of the errors in the data recorded by the meteorological stations in the country [2]. Furthermore, although the use of monthly averages is adequate for the sizing of preliminary equipment, daily, even hourly, values are generally required to design more precise facilities, such as when sizing solar absorbers [3]. Therefore, the recording of solar irradiation data, and its subsequent study are fundamental in contributing to the development of such technologies.

Another major problem encountered in global solar energy projects is the lack of maintenance and cleaning of both the solar panels and solar irradiation measuring instruments found in exposed outdoors locations. Solar measuring equipment requires periodic maintenance to avoid the accumulate dust as exposure to environmental conditions (wind, particulate matter, etc.) end up damaging the equipment, increasing the possibility of measurement errors and reducing the quality of the recorded data and/or the performance of the equipment, depending on the system [4]. The Atacama Desert, in which the Arica & Parinacota region is found, experiences irradiation which is unique in the world both in terms of the quality and quantity [5] This makes the area an attractive location for the development of solar energy projects. However, it also brings the problems typically associated with large deserts, those of large amounts of dust kicked up by winds causing the rapid fouling of the various solar infrastructures [6]. Darwish et al. 2015 describe that the dust is as any particulate matter less than 500 µm in diameter, which enters the atmosphere from different sources such as dust lifted by wind, vehicular exhaust, volcanic eruptions and air pollution. Pollen and also fungi, bacteria, vegetation, microfibers, and, most commonly, organic minerals such as sand, clay, and eroded limestone can be dust components in small portions [7], [8].

Possible sources of air pollutants are divided into two groups. On the one hand there are natural or biogenic particles and on the other, anthropogenic particles which are caused by human activity. The main sources of natural pollution are fugitive emissions from the soil, the surface of seas and oceans, volcanoes and biogenic emissions, consisting mainly of plant debris and microorganisms. In turn, natural contamination sources have secondary components, principally consisting of sulfates, nitrates and organic aerosols [9].

Anthropogenic sources of particulate matter are very diverse, mostly being found in urban, industrial and indoor areas. Traffic in urban areas is the main source of primary particles which come both from vehicle engine emissions (especially diesel) and the erosion of paving surfaces, brakes and tires [10]. The most commonly found air pollutants are: sulfur oxides (SO_X), nitrogen oxides (NO_X), carbon monoxide (CO), ozone (O_3), lead (Pb) and aerosols (which include settleable particles, particulate matter and fumes), etc. [11].

Several studies showed in the review of Saver et al., 2013 [12] report about the impact of dust on the use of solar energy in solar photovoltaic industry (PV) and concentrating solar-thermal power (CSP) generally for electricity generation. The main dust studies are related to sand and dust in the dessert climates and show that the constituents of the dust depend on the region and atmospheric conditions.

This review highlights that the applications of washing techniques for dust mitigation increase the operations and maintenance costs. In addition, in the dessert regions normally the main resource to wash (water) is scarce and this fact should be taken into account [12]. There are specific studies where the transmission degradation due to dust effects has been studied. Hottel and Woertz [13] observed that the dust accumulation on solar thermal system showed a 1% loss of efficiency on a glass plate, reporting a 4.7% maximum degradation. Dietz, 1963 [14] observed a reduction of 5% in the solar irradiation on glass due to the dirt accumulation. Hoffman and Ross [15] performed a laboratory study on PV module of glass encountering two field-related problems: surface soiling and encapsulated eliminating. Becker et al., 1997 [16] observed that the pollutions had an effect lower than 4% on PV operation. The list of this type of studies is very long, however it is very important to note that in all cases the studies were performed evaluating the PV and CSP materials showing that dust accumulation decreased the efficiency of the processes which causes depend on region (dirt or wet), tilt grade modules, material type modules (glass, plastic, etc.). However, very few studies [4] have focused on radiation measurement equipment. Therefore, the aim of this study was to evaluate the effect of environmental dirt on the global irradiation measurement equipment installed in a weather station in the city of Arica, Chile, as well as characterizing the content of the settleable particulate material deposited on the station.

2 Materials and Methods

2.1 Measurement Equipment

The weather station includes 3 pyranometers, 1 solar tracker, 1 temperature and relative humidity sensor and an anemometer. The specific brands and models of measuring equipment are shown in Table 1, while Figure 1 shows a photograph of the weather station. The station is located in the city of Arica, coordinates: 18.47° latitude south and 70.31° longitude west, at a height of 9 meters above sea level being specifically located on the roof of the Research Centre on Man in the Desert (CIHDE), located on the Velasquez campus of the University of Tarapaca.

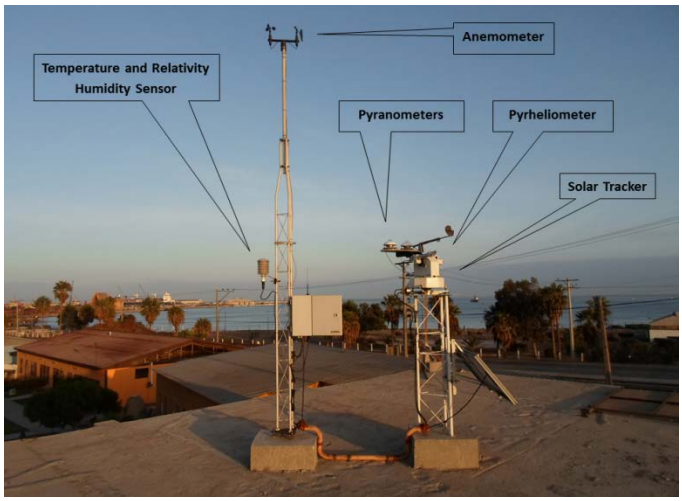

Figure 1. Weather station used in this study.

TABLE 1
EQUIPMENT IN THE WEATHER STATION: MANUFACTURERS, MODELS AND MEASUREMENTS

Instrument	Manufacturer	Model	Measurements
Pyranometer	Hukseflux Thermal Sensor	SR11	Global Horizontal Irradiation (W/m^2)
Pyranometer	Hukseflux Thermal Sensor	SR11	Diffuse Horizontal Irradiation (W/m^2)
Pyrheliometer	Hukseflux Thermal Sensor	DR01	Direct Normal Irradiation (W/m^2)
Solar Tracker	Geónica S.A. Ciencias de la Tierra	Solar Sun Tracker 3000	Sun Elevation and Orientation (º)
Temperature and Relativity Humidity Sensor	Geónica S.A. Ciencias de la Tierra	STH-5031 (TA/HR)	Temperature (ºC) and Relativity Humidity
Anenometer	Wind Sentry	03002	Wind Speed (m/s) and Direction (º)

2.2 Data Acquisition

In order to be able study the effect that dirt (deposition of settleable particulate material) has on the global irradiation measurements taken by a pyranometer, it is necessary to obtain real values of global irradiation even when dirt begins to accumulate on the pyranometer. Since the team also has direct and diffuse solar irradiation meters, the first part of this study (Clean Phase) consisted of obtaining a model of the global solar irradiation from direct and diffuse irradiation data. During this

- *1 Laboratory for Environmental Research in Arid Zones, LIMZA, School of Mechanical Engineering, University of Tarapacá, Arica, Chile. E-mail: lorenacp@uta.cl - lorenacornejop@gmail.com*
- *2 Centre for Research on Man in the Desert, CIHDE, Arica, Chile*
- *3 School of Mechanical Engineering, EUDIM, University of Tarapacá, Arica, Chile*

period, between 1 and 8 June 2014, all the instruments that make up the station were cleaned daily to allow the validity of the model to be studied. Once this phase was completed, the second measurement phase (Dirty Phase) was carried out between 12 and 26 June 2014, during which, in order to study the effect of dirt, all instruments in the meteorological station were properly cleaned with the exception of the pyranometer used to measure global solar irradiation.

The acquisition of data was based on Coordinated Universal Time (UTC-5), which is the standard principle of time which regulates clocks in the world and uses the Greenwich meridian as the zero reference. Although the weather station acquired data continuously 24 hours a day, the solar irradiation was analysed between 06:30 and 17:20 (sunrise and sunset respectively). The weather station is capable of taking measurements each minute but, to facilitate data processing, a sampling time of 10 minutes with the average of the data recorded in that period of time being used as the data point for further analysis.

2.3 Selection of the mathematical model

To study the effect of dirt on the global irradiation measurements obtained by a pyranometer it is necessary compare the real values and the modified values obtained as a result of the loss of equipment sensitivity. Since it was not possible to use two pyranometers simultaneously in the elaboration of this research, the first step was to obtain a model of global irradiation using the other data available from the weather station as input variables.

Global solar irradiation can be calculated as the sum of direct and diffuse components; data which may also be provided by the weather station. Thus, the initial objective of the first phase was to compare measurements from the pyranometer (global irradiation) with the sum of the measurements from the pyrheliometer (direct irradiation) and a second pyranometer coupled with a shaded ring (diffuse irradiation), as described in Equation 1:

$$G(\beta,\alpha)_{calculated} = B(\beta,\alpha) + D(\beta,\alpha) \quad (1)$$

Where $G(\beta,\alpha)_{calculated}$ is the global irradiation incident on an inclined surface at an angle corresponding to (β,α), $B(\beta,\alpha)$ is the direct irradiance on an inclined surface at an angle of (β,α) and $D(\beta,\alpha)$ is the diffuse irradiance on an inclined surface at an angle of (β,α). Likewise β represents the inclination of a surface with respect to the horizontal and α the azimuth of a surface with respect to midday.

Values for global irradiation measured by the radiometer and global irradiation calculated as the sum of the components can be compared for two days in the first phase in Figure 2. The results of the two values are very similar, as expected, however, certain differences are apparent as is reflected in the error curve obtained from Equation 2.

$$Error\ (\%) = \left|\frac{G(\beta,\alpha)_{calculated} - G(\beta,\alpha)_{measured}}{G(\beta,\alpha)_{measured}}\right| \cdot 100 \quad (2)$$

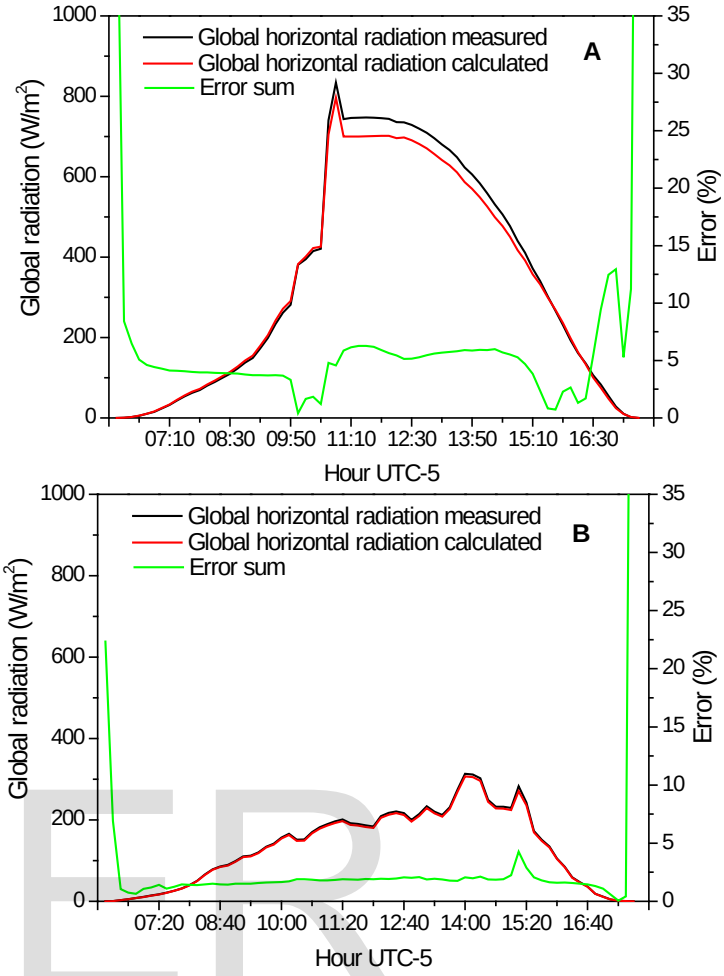

Figure 2. Comparison of measured and calculated global irradiation for June 1, 2014 (A) and on June 7, 2014 (B). Data corresponding to the first phase. The error between the two figures is also shown.

Where $G(\beta,\alpha)_{calculated}$ represents global solar irradiation calculated as the sum of the direct and diffuse components while $G(\beta,\alpha)_{measured}$ represents the measurement taken directly by the pyranometer.

The characteristics of the error are common to each day (see Figure 2-A and a-B). At either extreme, corresponding to the early hours of the morning and late afternoon, higher errors are observed when the values of irradiation are extremely low. This is to be expected since, when the error is standardised a small deviation in the measurements leads to very high percentages. Moreover, it can be seen that during the course of the day the error moves within a range of values depending on the level of solar irradiation. When the irradiance is noticeable but low, for example due to the presence of clouds, there is an error of around 1.5-2.0% while at the solar midday and in sunny conditions, the percentage rises to almost 6%. It should be noted that the error increases as the sun sets, something observed on every day evaluated. When the irradiance falls below 200 W/m2 in the evening as a consequence of the beginning of the sunset, the deviation increases to values above 10% but later returns to expected levels (Figure 2-A). Given that the same

pyranometer is used to measure the diffuse component and the global irradiation, it is likely that the error is caused by the pyrheliometer.

In order to improve results and reduce the errors described above, it was decided to apply a mathematical model using the values of direct and diffuse irradiation as its input variables. Consequently, a polynomial equation was formed in the order was varied; the coefficient of determination (R^2), the mean square error (RMSE) and statistical bias (MBE) were used as selection parameters to find the most accurate equation (Equations 3 and 4, respectively) and whose results are shown in Table 2.

TABLE 2
VALUES OF STATISTICAL PARAMETERS RESULTING FROM THE APPLICATION OF DIFFERENT PROPOSED MATHEMATICAL MODELS

Equation	R^2	RMSE (W/m^2)	MBE (W/m^2)
1st order	0.9993	22.7 (8.4%)	14.8 (5.4%)
2nd order	0.9994	22.4 (8.2%)	14.8 (5.4%)
3rd order	0.9994	29.4 (10.8%)	18.9 (6.9%)
4th order	0.9994	15.4 (5.7%)	10.4 (3.8%)
5th order	0.9995	52.8 (19.8%)	31.9 (11.9%)
6th order	0.9995	59.7 (21.9%)	-28.9 (-10.6%)

$$\text{RMSE}=\sqrt{\frac{1}{N}\sum_{i=1}^{N}\left(G(\beta,\alpha)_{measured_i}-G(\beta,\alpha)_{calculated_i}\right)^2} \quad (3)$$

$$\text{MBE}=\frac{1}{N}\sum_{i=1}^{N}\left(G(\beta,\alpha)_{measured_i}-G(\beta,\alpha)_{calculated_i}\right) \quad (4)$$

The coefficient of determination is the same for all the proposed equations and effectively equals 1. As such, the parameters RMSE and MBE had to be used to choose the most representative model. The first and second order equations obtained very similar values (around 8% and 5.4% for RMSE and MBE respectively). The third order equation gives errors which are slightly higher than those of the lower-order equations, while the fourth order equation obtained the best results with an RMSE of 5.7% and MBE of 3.8%. The rest of the equations gave considerably larger errors and thus were immediately discarded. Equation 5 shows the selected polynomial including values of the respective parameters which resulted from the adjustment process of the model.

$$G(\beta,\alpha)_{model}=-2*10^{-10}G(\beta,\alpha)^4_{calculated}+1*10^{-7}\,G(\beta,\alpha)^3_{calculated}+\quad+0{,}0001G(\beta,\alpha)^2_{calculated}+0{,}9923G(\beta,\alpha)_{calculated}+0{,}989 \quad (5)$$

Where $G(\beta,\alpha)_{model}$ represents the global irradiation calculated by the model.

To determine whether the use of the mathematical model represents an improvement over the direct calculation of the global irradiation obtained by summing the direct and diffuse components, the error in the accumulated global solar irradiance was calculated for each day of the first phase by both methods and then compared. As is reflected in Table 3, the use of the model allows the error to be reduced. In fact, one of the improvements observed is the correction of the overestimation which occurs during sunset (Figure 2-A and 2-B) which, as has been mentioned above, is an error common to most of days studied. The only day on which a better prediction is achieved by calculating the sum of the components corresponds to the day with the least average irradiation, assuming a similar error in both methods.

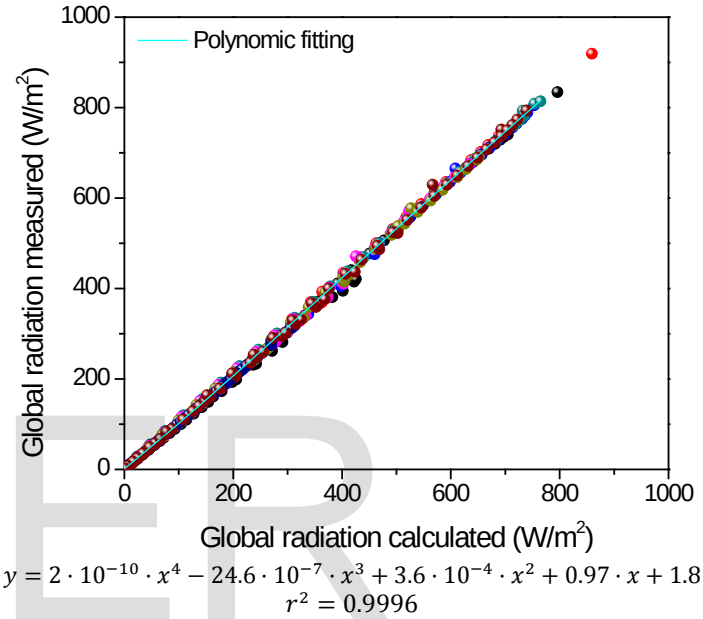

Figure 3. Calibration curve using the values of the global calculated irradiance measured by the pyranometer using the data from first phase.

TABLE 3
COMPARISON OF AVERAGE GLOBAL IRRADIATION ERROR IN THE CLEAN PHASE CAUSED BY THE SUMMATION OF COMPONENTS AND THE MODEL

Day	Average Irradiation Measurement	% error Summation of components	% error Model
01/06/2014	342.96	3.90	3.86
02/06/2014	297.15	5.72	3.56
03/06/2014	303.02	5.06	3.71
04/06/2014	274.72	5.31	3.53
05/06/2014	210.80	4.79	3.51
06/06/2014	234.89	4.58	3.61
07/06/2014	134.14	1.94	2.18
08/06/2014	314.95	5.05	3.82

Consequently, due to its greater precision, the mathematical

model was chosen for the second phase of this work which involves the study of sensitivity loss of the global irradiation measuring equipment as a result of the effect of accumulation of particulate matter on the surface of the pyranometer.

2.4 Characterization of settleable particulate material

With the aim of determining the sources of pollution that affect the radiometric station, a characterisation study of settleable particulate matter was conducted.

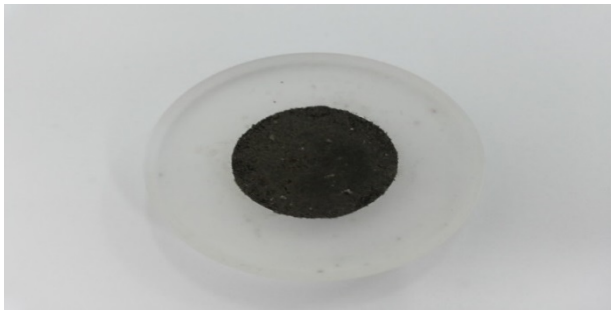

Figure 4. Sample of settleable material from the weather station.

A sample of settleable particulate matter which had adhered directly to the station was collected (Figure 1) using the method described by Ram et al. 2014 [S.S. Ram, R.V. Kumar, P. Chaudhuri, S. Chanda, S.C. Santra,M. Sudarshana, A. Chakraborty, Physico-chemical characterization of street dust and re-suspended dust on plant canopies: An approach for finger printing the urban environment, Ecological Indicators 36 (2014) 334– 338], making sure that the surface from which the sample is taken was free from foreign matter (such as rusted structural metal, peeling paint or animal or bird faeces, etc.) that might interfere with the subsequent analysis. In the recollection of the samples, a clean brush with a width of approximately 10 centimetre was used to gather the settleable matter. Subsequently, it was placed in a sealed polyethylene bag.

The settleable particulate matter sample (Figure 4) was characterised by Bruker-AXS model D2-Phaser X-ray diffraction equipment (XRD) whose operating principle is based on the interaction of a solid with a source of X-rays under certain instrumental conditions (Table 4). This instrument provides a diffraction pattern which, by means of a database, is used to evaluate the phases.

TABLE 4
INSTRUMENTAL CONDITIONS IN THE XRD ANALYSIS OF SETTLEABLE PARTICULATE MATTER ADHERED TO THE VELAZQUEZ RADIOMETRIC STATION BY MEANS OF DISPERSION

Parameter	Details
Goniometer	Vertical Bragg-Bretano
Irradiation	Cu k_{a1} (I = 1.5406 $\hat{A}$)
Voltage	30 Kv
Intesity	30 mA
Detector	Xflash
Monochromator	Kβ-Filtro, ROI (Xflash)
Slits	1 mm/1 mm/0.6 mm
Scan Range	3 – 80° 2θ
Step Size	020° 2θ
Step Time	1.0 s
Data Base	COD (Crystallography Open Database)
Quantifier Program	TOPAS (Total Pattern Analysis Software)

The analysis of samples consisted of the evaluation of the mineral phases by means of ".EVA"software which identifies the crystalline phases in a solid sample by means of a database. A software called "TOPAS" was used to analyse the content of the determined mineral phases by carrying out a semi quantitative analysis of the diffractogram using the information provided by the ".EVA" program.

3 Results and Discussion

Global irradiance values are calculated from the direct and diffuse irradiation data taken in the period from June 12 until June 26, 2014 (Dirty Phase) and, using the model obtained (Equation 5).

Firstly, daily error curves were individually studied to determine if there is a relationship between the level of irradiance and the error so as to take this aspect into account when analysing sensitivity loss due to the particulate matter deposited on the surface of the pyranometer. Three different areas can be identified in the relationship between the irradiance value and the error (see Figure 6): (i) when irradiation is below 50 W/m2, during the first and last moments of sunlight, the largest percentage errors occur although they are smaller if they are expressed in absolute terms (ii) when the irradiance value is between 50 and 500 W, approximately, W/m2, the error in both relative and absolute terms increases with increasing irradiance (iii) above 500 W, approximately, W/m2 the error curve becomes saturated and the value stabilises at around 5-6% while, when the irradiance increases above 700 W/m2, the error decreases slightly.

Therefore, during sunny days, the error remains very stable after reaching a certain level of irradiation and for long periods of time around the solar noon (see Figure 6-A). Conversely, on days with considerable cloud presence, and therefore with unstable global irradiance levels, normally below 500 W/m2, the error is smaller but much more variable (see Figure 6-B).

Figure 7 describes the average error evolution over the days studied in this second phase. Until the eighth day errors are within a range of 2 to 2.5 % and then increase steadily to 4.2 % on the tenth day. During the first 8 days the value of average global irradiance remains fairly stable, which, in theory, should keep the error within a narrow range. As this is shown to be true, it can be inferred that the effect of dirt is negligible. After the 8th day the error increases even when the average daily irradiation value decreases, which should theoretically lower the error. This indicates that the material deposited on the surface of the pyranometer has begun to have a noticeable effect on readings. During the 11th and 12th days there is a slight decrease in the mean error before it finally increases to its

highest values during this study, reaching almost 5%. The decrease on the eleventh and twelfth days coincides with a rise in global irradiance which could indicate that the particulate material has a greater influence at low irradiation levels. It should be noted that throughout this work irradiance levels lower than 5 W/m2 were discarded in order to avoid the influence of errors corresponding to the rising and setting of the sun, which surpass 100%.

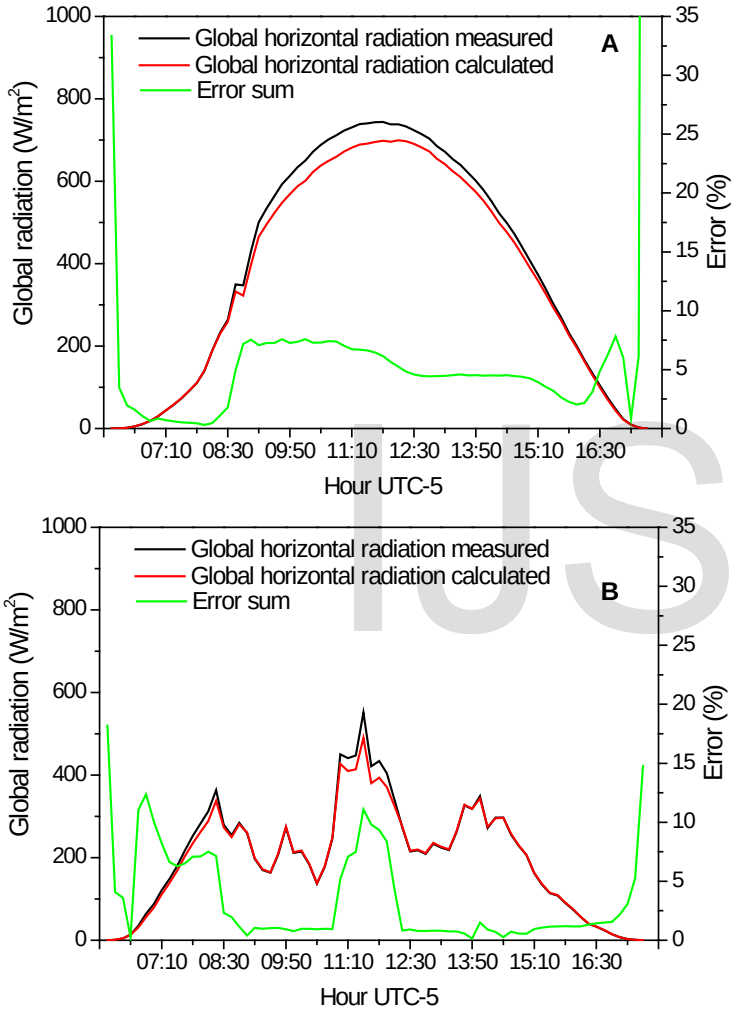

Figure 6. Comparison of theoretical and measured global irradiation (dirty phase) and the error curve which correspond to July 18, 2014 (A) and 20 June 2014 (B).

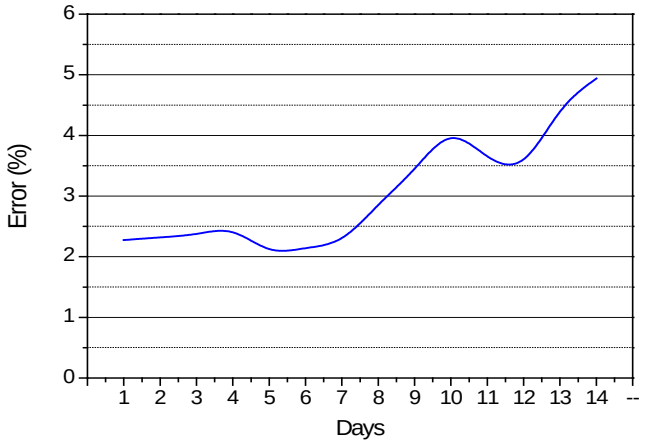

Figure 7. Error evolution over the Dirty Phase period.

The mineral phases present in the largest quantities in the XRD analysis of the sample of settleable particulate matter taken from the weather station were: Halite, Gypsum, Quartz, Albite, Anorthite and Anhydrite (Table 5).

TABLE 5
MINERAL PHASES OBTAINED BY XRD FROM THE SAMPLE OF SETTLEABLE PARTICULATE MATERIAL

Content	Category	Formula	Percentage Contents (%)
Halite	Halide Mineral	$NaCl$	38.2
Gypsum	Sulfate Minerals	$CaSO_4 \cdot 2H_2O$	14.2
Quartz	Silicate Mineral	SiO_2	14.3
Albite	Tectosilicate Minerals	$NaAlSi_3O_8$	18.2
Anorthite	Feldspar Mineral	$CaAl_2Si_2O_8$	11.9
Anhydrite	Sulfate Minerals	$CaSO_4$	1.3

Table 5 shows the XRD analysis of the settleable particulate material sample adhered to the station by means of dispersion. The mineral phase found in the greatest proportion in the inorganic fraction was Halite which made up 38.2% of all minerals. This mineral is abundant in marine atmospheres, where salt water constitutes the basic source of mineralised particles. As such, its origin is mainly associated with marine sources.

Another important mineral present is quartz, one of the main constituents of the earth's crust. Quartz is found in almost all mineralogical environments and is a predominant component of rock types, which means it is normally associated with naturally occurring sources. Gypsum, Anorthite, Anhydrite and Albite are commonly found as clays and may be present as a

result of construction earthworks or originate geologically through particulate dispersion.

It is common for an abundance of quartz and clay minerals to collect in places where traffic does not have a major impact. Consequently, it can be inferred that the majority of contamination deposited on the station originates from marine and geological sources.

4 Conclusions

In the present study, the effect the accumulation of particulate matter on the surface of a pyranometer has on the measurements of global solar irradiation was studied while said matter is characterized by means of RDX.

Calculating global irradiation by adding the direct and diffuse components is an effective method (4.5% average error), although the use of a polynomial equation allows this error to be reduced (3.5% average error). The fourth order polynomial obtained the best results, with a coefficient of determination of 0.994 and RSME and MBE values of 5.7% and 3.8% respectively.

It was observed that the error in the measurement is related to the irradiation level and the presence of three characteristic zones: (i) when irradiatiance is below 50 W/m2 the largest errors are present (ii) when irradiance is between 50 and 500 W/m2 the error increases as irradiance increases (iii) above 500 W/m2 the error stabilises in the region of 5-6%. In addition, it was determined that the effect of dirt is negligible during the first 7 days. Therefore, it is recommended that for the proper functioning of this equipment in areas with similar climate conditions to those of the Arica & Parinacota region, cleaning periods of no more than one week should be established.

By studying characterisation of particulate matter in the samples collected at the station, the minerals present in greatest proportions were identified as: Halite, Gypsum, Quartz, Albite, Anorthite and Anhydrite. All these minerals appear to be originate from natural sources of contamination such as the proximity to the Pacific Ocean and the desert conditions in the area. No mineral that may be associated with anthropogenic sources was found in any great quantity. This leads to the conclusion that the contaminants which most affect the collection of data at the station come from natural sources.

Acknowledgment

The authors would like to thanks the Centre for Research on Man in the Desert, CIHDE (www.cihde.cl) for access to the radiometric station, Conicyt/FONDAP/15110019 for the financial support for this project and the Laboratory for Environmental Research in Arid Zones, LIMZA (http://limza.uta.cl/) for the use of its premises. Alejandro Cabrera would like to thank SERC Chile (Conicyt/FONDAP/15110019) for his postdoctorate position.

References

[1] M. Shaddel, D. S. Javan, P. Baghernia, "Estimation of Hourly Global Solar Irradiation on Tilted Absorbers from Horizontal one Using Artificial Neural Network for Case Study of Mashhad", *Renewable and Sustainable Energy Reviews*, vol. 53, pp. 59-67, January 2016, ISSN 1364-0321.

[2] A. Ortega, R. Escobar, S. Colle, Samuel Luna de Abreu, "The State of Solar Energy Resource Assessment in Chile", Renewable *Energy,* vol. 35, pp. 2514-2524, 2010

[3] A. Lecontea, G. Achard, "Solar Combisystem Characterization with a Global Approach Test and a Neural Network Based Model Identification", Energy Procedia, vol 30, pp. 1322–1330, SHC 2012

[4] G. Stanhill, "Accuracy of Global Irradiation Measurements at Unattended, Automatic Weather Stations", *Agricultural and Forest Meteorology*, vol. 61, pp. 151-156, 1992

[5] R. Escobar, A. Ortega, C. Cortés, A. Pinot, E. B. Pereira, F. R. Martins, John Boland, "Solar Energy Resource Assessment in Chile: Satellite estimation and ground station measurement", *Energy Procedia*, vol. 57, 1257 – 1265, 2014

[6] K. Al Khuffasha, L. A. Lamontb, L. El Chaarc, "Analyzing the Effect of Desert Environment on the Performance of Photovoltaics", , Applied Solar Energy, vol. 50, No. 4, pp. 215–220. © Allerton Press, Inc., 2014, ISSN 0003-701X

[7] R.A. Bagnold, "The physics of blown sand and desert dunes", *Courier Dover Publications*; 2012, www.doverpublications.com

[8] Z.A. Darwish, H.A. Kazem, K. Sopian, M.A. Al-Goul, H. Alawadhi, "Effect of dust pollutant type on photovoltaic performance" *Renewable and Sustainable Energy* Reviews, vol. 41, pp. 735-744, 2015

[9] R.A. Sutherland, C.A. Tolosa, "Multi-element analysis of road-deposited sediment in an urban drainage basin, Honolulu, Hawaii", Environmental Pollution, vol. 110, pp. 483-495, 2000

[10] M. Guney, T. T. Onay, N. K. Copty, "Impact of overland traffic on heavy metal levels in highway dust and soils of Istanbul, Turkey", *Environmental Monitoring and Assessment,* vol. 164, pp. 101–110, 2010

[11] S.S. Ram, R.V. Kumar, P. Chaudhuri, S. Chanda, S.C. Santra,M. Sudarshana, A. Chakraborty, "Physico-chemical characterization of street dust and re-suspended dust on plant canopies: An approach for finger printing the urban environment", *Ecological Indicators,* vol. 36, pp. 334– 338, 2014

[12] T. Sarver, A. Al-Qaraghuli, LL. Kazmerski, "A comprehensive review of the impact of dust on the use of solar energy: history, investigations, results, literature, and mitigation approaches", *Renewable Sustainable Energy* Reviews, vol. 22, pp. 698–733, 2013

[13] H.C. Hottel, B.B. Woertz, "The performance of flat plate solar heat collectors", *ASME Transantions,* vol. 64, pp. 91-104, 1942

[14] A.G.H. Dietz, "Diathermanous materials and properties of surface", A.M. Zarem, D.D. Erway editors, *Introduction to the utilization of solar energy*, pp. 59-86, New York 1963

[15] A.R. Hoffman, R.G. Ross Jr., "Environmental qualification testing of terrestrial solar cell modules", *Proceeding of the conference record of the thirteenth IEEE photovoltaic specialists conference*, pp. 835-842, 1978

[16] H. Becker, W. Vaaben, W. Heerman, "Reduced output of solar generators due to pollution", *proceedings of the 14th European photovoltaic solar energy conference*, Barcelona 1997

[17] D. Feuermann, A. Zemel, "Dust-induced degradation of pyranometer sensitivity", *Solar Energy,* vol. 50, No. 6, pp. 483-486, 1993

[18] D. Faiman, D. Feuermann, A. Zemel, "Accurate field calibration of pyranometers", *Solar Energy*, vol. 49, No 6, pp. 489-492, 1992

[19] World Meteorological Organisation, "Guide to Instruments and Methods of Observation", *WMO N°8,* Geneva, Switzerland. Sixth Edition, 1996

[20] M.C. Kotti, A.A. Argiriou, A. Kazantzidis, "Estimation of direct normal irradiance from measured global and corrected diffuse horizontal irradiance", *Energy,* vol. 70, 382-392, 2014